sustainability

MDPI

Article

Transmission Factor (TF) Behavior of Bi_2O_3–TeO_2–Na_2O–TiO_2–ZnO Glass System: A Monte Carlo Simulation Study

Huseyin O. Tekin [1,2], Ghada ALMisned [3], Gulfem Susoy [4], Fatema T. Ali [5], Duygu Sen Baykal [6], Antoaneta Ene [7,*], Shams A. M. Issa [8,9], Yasser S. Rammah [10] and Hesham M. H. Zakaly [9,11,*]

1 Medical Diagnostic Imaging Department, College of Health Sciences, University of Sharjah, Sharjah 27272, United Arab Emirates; htekin@sharjah.ac.ae
2 Computer Engineering Department, Faculty of Engineering and Natural Sciences, Istinye University, Istanbul 34396, Turkey
3 Department of Physics, College of Science, Princess Nourah Bint Abdulrahman University, Riyadh 11671, Saudi Arabia; gaalmisned@pnu.edu.sa
4 Department of Physics, Faculty of Science, Istanbul University, Istanbul 34134, Turkey; glfmsusoy972@gmail.com
5 Center for Advanced Materials Research, Research Institute of Sciences and Engineering, University of Sharjah, Sharjah 27272, United Arab Emirates; fatema.taleb98@gmail.com
6 Vocational School of Health Sciences, Medical Imaging Techniques, Istanbul Kent University, Istanbul 34433, Turkey; duygu.sen@kent.edu.tr
7 INPOLDE Research Center, Department of Chemistry, Physics and Environment, Faculty of Sciences and Environment, Dunarea de Jos University of Galati, 47 Domneasca Street, 800008 Galati, Romania
8 Physics Department, Faculty of Science, University of Tabuk, Tabuk 47512, Saudi Arabia; sh_issa@ut.edu.sa
9 Physics Department, Faculty of Science, Al-Azhar University, Assiut 71524, Egypt
10 Department of Physics, Faculty of Science, Menoufia University, Shebin El-Koom 32511, Egypt; dr_yasser1974@yahoo.com
11 Institute of Physics and Technology, Ural Federal University, 620002 Ekaterinburg, Russia
* Correspondence: antoaneta.ene@ugal.ro (A.E.); h.m.zakaly@gmail.com or h.m.zakaly@azhar.edu.eg (H.M.H.Z.)

Abstract: The main objective of the present work was to assess the gamma radiation shielding competencies and gamma radiation transmission factors (TFs) for some tellurite glasses in the form of Bi_2O_3–TeO_2–Na_2O–TiO_2–ZnO. MCNPX general-purpose Monte Carlo code (version 2.6.0) was utilized for the determination of TF values at various well-known radioisotope energies for different glass thicknesses from 0.5 cm to 3 cm. Moreover, some important gamma ray shielding properties were also determined in the 0.015–15 MeV energy range. The results show that glass densities were improved from 5.401 g/cm^3 to 6.138 g·cm^3 as a function of Bi_2O_3 increment in the glass composition. A S5 glass sample with the maximum Bi_2O_3 additive was reported with superior gamma ray shielding properties among the studied glasses. It can be concluded that Bi_2O_3 can be used as a functional tool in terms of improving glass density and, accordingly, gamma ray shielding attenuation properties of tellurite glasses, where the role Bi_2O_3 is also critical for other material properties, such as structural, optical, and mechanical.

Keywords: Bi_2O_3–TeO_2–Na_2O–TiO_2–ZnO glass system; radiation shielding; MCNPX

check for updates

Citation: Tekin, H.O.; ALMisned, G.; Susoy, G.; Ali, F.T.; Baykal, D.S.; Ene, A.; Issa, S.A.M.; Rammah, Y.S.; Zakaly, H.M.H. Transmission Factor (TF) Behavior of Bi_2O_3–TeO_2–Na_2O–TiO_2–ZnO Glass System: A Monte Carlo Simulation Study. *Sustainability* **2022**, *14*, 2893. https://doi.org/10.3390/su14052893

Academic Editor: Antonio Caggiano

Received: 23 January 2022
Accepted: 28 February 2022
Published: 2 March 2022

Publisher's Note: MDPI stays neutral with regard to jurisdictional claims in published maps and institutional affiliations.

1. Introduction

Lead-based glasses have historically been used for γ-ray radiation shielding and protection against other ionizing human harmful radiation due to their broad physical and chemical properties. Owing to their poisonous nature, lead-based glasses are no longer widely used in many radiation shielding applications. Many attempts to replace them with lead-free materials or radiation-shielding glasses have been documented in the literature. Heavy metal oxide-based glasses, such as bismuth oxides, are examples of these materials that have already had an influence and relevance in many industrial applications [1,2]. At present, different materials engineers and shielding material developers are focusing

on producing shielding materials that are flexible, light, environmentally friendly, and inexpensive against gamma rays. As a result, glasses are a good alternative to standard protective materials since they have intriguing optical and physical properties and can be easily manipulated with any chemicals and production methods [3–5]. Construction, design engineering, optical telecommunications, and radiation protection are just a few of the applications for glasses. In circumstances when concrete or other materials such as polymers or metals fail, glasses can be utilized as a protective layer. Different research groups have since explored tellurite, lithium borate, silicate, lead fluoroborate, bismuth-borate, commercial glasses, and zinc borotellurite glasses for their possible use as photon shielding materials [6–12]. Tellurium dioxide (TeO_2) is the most stable oxide of tellurium. The researchers decided to use tellurium oxides in glasses because of their stability. Tellurium glasses are noncrystalline solids that have many applications in different chemical compositions and temperatures and are used in binary, triple, and quaternary glass systems containing transition metal or rare earth oxides. Because of its potential utility in the fields of fuel cells, optical amplifier solid-state batteries, and eventually non-linear optical microdevices, tellurium oxide-based glasses have received a lot of attention in both basic science and engineering [13]. Therefore, tellurite-based glasses have become a popular subject of study, ranging from basic Raman and IR spectra through optical characteristics and differential scanning calorimetry to thermal parameters [13–16]. They also have a lower mean free path than concrete and some commercial glasses. As a result, tellurite-based glasses are a good choice for a variety of technological applications, such as optical memories, optical devices, optical amplifiers, glass fibers, optical sensors, solar cells, laser writing, telecommunications, optoelectronics, photonics, gamma ray protection, and radiation shielding glasses [17–20]. Tellurite glass is a conditional glass form in which tellurium is unable to self-construct glass. Pure TeO_2 is unstable and crystallizes rapidly due to the lone electron pair located in the equatorial position of the TeO_4 units. As a consequence, the structural rearrangement of these units is severely regulated throughout the glass forming process. To enhance the glass forming capabilities of the tellurium oxides, modifier oxides such as alkali, alkaline, or heavy metal oxides must be added to the composition. ZnO and Na_2O are two modifier oxides that are often used to increase the stability of glass and prevent it from crystallizing [21–24]. Sultana et al. [25] established a sustainable and repeatable process for producing zinc oxide (ZnO), as well as its use in photocatalytic degradation of organic contaminants. A combination of extremely porous sawdust and zinc nitrate hexahydrate was combusted at 600 °C to produce ZnO in a tube furnace. Because of its uses in cosmetics, medicine, as an antibacterial agent, and as catalysts, zinc oxide (ZnO) is one of the nanoscale materials with rapidly rising production [26]. The introduction of zinc oxide (ZnO) into aquatic environments through home and industrial wastewaters has the potential to harm fish and other creatures. The hazardous potential of several metal-based nanomaterials has raised growing concerns about the environmental threat to aquatic biota. Size, shape, surface charge, and aggregation state of ZnO all have a role in biological impacts, such as genotoxic, mutagenic, and cytotoxic effects. Beegam et al., 2016 [26] found Zn bioaccumulation, histological, and hematological alterations in ZnO-exposed mice as a result of oxidative and cellular stress. Tellurite-based glasses may also benefit from the addition of high atomic weight enhancer oxides such as lead oxides (PbO) and bismuth oxides (Bi_2O_3), which improve the refractive index and transmission windows while also broadening the infrared (IR) spectrum. Additionally, glasses containing heavy metal oxide modifiers such as Bi_2O_3, PbO, and Ga_2O_3 have been reported to have a high density, a high refractive index, and highly nonlinear optical characteristics, making them attractive applicants for photonic materials, signal processing, and communication device development [24]. The addition of a tiny amount of TiO_2 to a glass batch improves chemical stability and glass-forming ability. When a small amount of transition metal oxides is added to batches of glass-like TiO_2, however, the glass network changes dramatically, causing detectable changes in the physical properties of the glasses [27,28]. Bismuth oxide

(Bi_2O_3) plays an important role in semiconducting glasses, and it can be used to improve the properties of glass formers [29–31].

The main objective of the present work is to assess the gamma radiation shielding competencies and gamma radiation transmission factors (TFs) for tellurite glasses in the form of Bi_2O_3–TeO_2–Na_2O–TiO_2–ZnO. This objective was achieved by using the Phys-X/PSD program and MCNPX Monte Carlo simulations. The findings of this study and the discrepancies in material behavior caused by chemical composition changes may contribute to the improvement of the operational conditions for heavy metal oxide-reinforced shielding glasses, which have the potential to be used in applications such as diagnostic radiology, nuclear medicine, nuclear reactors, and nuclear waste management.

2. Materials and Methods

2.1. Materials

Five samples of bismuth–tellurite–sodium–titania–zinc with chemical formula xBi_2O_3-(80-x)TeO_2-5Na_2O-5TiO_2-10ZnO, where x = 5–15 mol% were selected from previous Ref. [31]. The investigated glasses were formed and named as:

$5Bi_2O_3$-75TeO_2-5Na_2O-5TiO_2-10ZnO (**S1**), $8Bi_2O_3$-72TeO_2-5Na_2O-5TiO_2-10ZnO (**S2**), $10Bi_2O_3$-70TeO_2-5Na_2O-5TiO_2-10ZnO (**S3**), $12Bi_2O_3$-68TeO_2-5Na_2O-5TiO_2-10ZnO (**S4**), and $15Bi_2O_3$-65TeO_2-5Na_2O-5TiO_2-10ZnO (**S5**). Sample code, elemental weight fraction, and density of the Bi_2O_3–Na_2O–TiO_2—ZnO–TeO_2 glasses are tabulated in Table 1.

Table 1. Samples code, elemental weight fraction, and density of Bi_2O_3–Na_2O–TiO_2–ZnO–TeO_2 glasses.

Sample Code	Elemental Weight Fraction (wt%)						Density (g/cm^3)
	Te	O	Zn	Ti	Na	Bi	
S1	0.6048	0.1921	0.0413	0.0151	0.0145	0.1321	5.401
S2	0.5488	0.1844	0.0391	0.0143	0.0137	0.1997	5.613
S3	0.5147	0.1798	0.0377	0.0138	0.0132	0.2408	5.762
S4	0.4829	0.1754	0.0364	0.0133	0.0128	0.2791	5.844
S5	0.4392	0.1694	0.0346	0.0127	0.0122	0.3320	6.138

2.2. Gamma Ray Shielding Parameters

2.2.1. Linear Attenuation Coefficient (μ, cm^{-1})

In the field of radiation experimental research, the relation between the counts of attenuated gamma rays I(x) and the counts of the unattenuated gamma rays $I_o(x)$ through a material of thickness (x) is given as [32]

$$I(x) = I_o e^{-\mu x} \quad (1)$$

where μ is the probability of total interaction per unit thickness in a shield material and called linear attenuation coefficient in cm^{-1}.

2.2.2. Tenth Value Layers ($X_{1/10}$, cm)

The tenth value layer ($X_{1/10}$) is the material thickness required to reduce the primary value of counts of photons by one tenth; it measures in cm and can be given as [33]

$$X_{1/10} = \frac{\ln(10)}{\mu} \quad (2)$$

2.2.3. Total Atomic Cross Sections, ACS (σ_T)

The probability of interactions between primary photons and composite atoms is called the ACS, (σ_T) and can be evaluated as a function of mass attenuation coefficient, (μ/ρ) as [33]

$$\sigma_T = \left(\frac{\sum_i f_i A_i}{N_A}\right).\left(\frac{\mu}{\rho}\right) \text{ barns/atom or cm}^2/\text{g} \quad (3)$$

where N_A is the Avogadro's number, $\sum_i f_i A_i$ is the atomic mass of the composite, A_i is the atomic mass of the ith element in the composite. f_i denotes the mole fraction of the ith element with respect to the number of atoms.

2.2.4. Total Electronic Cross Sections, ECS (σ_e)

The ECS (σ_e) is a parameter that indicates the probability of interactions between primary photons and composite electrons and can be evaluated as [33]

$$\sigma_e = \left(\frac{1}{N_A}\right) \sum_i \left[\frac{f_i A_i}{Z_i}\left(\frac{\mu}{\rho}\right)\right] \text{ barns/atom or } cm^2/g \quad (4)$$

where Z_i is the atomic number of the ith element.

2.2.5. Effective Atomic Number (Z_{eff})

The effective atomic number is a parameter affected by Compton scattering interaction process of the composite and can be calculated as [34]

$$Z_{eff} = \frac{\sigma_T}{\sigma_e} \quad (5)$$

All radiation shielding parameters (μ, $X_{1/10}$, σ_T, σ_e, and Z_{eff}) were evaluated in the present work via Phy-X/PSD software [35].

2.3. MCNPX Monte Carlo Simulations for Transmission Factor (TF) Calculations

Along with basic gamma ray shielding characteristics, it is critical to evaluate the shielding materials' specific attenuation capabilities when primary and secondary gamma rays are present. This method may offer critical information on the percentage of gamma rays transferred via shielding material. The term transmission factor (TF) [36] is a critical metric that may aid in finding the aforementioned values in order to acquire a better knowledge of the attenuation properties of shielding materials against ionizing gamma rays. The transmission factor (TF) of the examined glasses was estimated in this research utilizing the MCNPX [37] (version 2.7.0) Monte Carlo simulation code. The TF value assigned to a particular absorber was the radiation flux (F) ratio traveling through the material medium to the flux incident on the absorber's surface. We calculated the TF of the examined glasses by dividing the mean gamma ray flux in the F4 tally mesh by the mean gamma ray flux in the uniform detection field. To convert this formulation into MCNPX code, two detection fields were positioned in front and behind the glass. While the intensity of primary gamma rays was measured in the detection zone just in front of the glass material, the intensity of attenuated gamma rays traveling through the glass was observed in the detection region directly behind the glass. Figure 1 illustrates the MCNPX simulation setup for the gamma ray transmission factor. The transmission factor (TF) measurement geometry was modelled using the code's INPUT file as a first step in the simulation technique. The INPUT file of MCNPX is composed of three major components: a CELL card, a SURFACE card, and a DATA card. To start, we determined the CELL structures of the equipment by measuring their covering surfaces and densities. Additionally, the CELL card component also includes material IDs (Mn). Following that, the geometrical alignments of the surfaces for the TF configuration were entered, as well as their geometrical structures, which may be planar, spherical, or cone. We included radioisotope energies and the source geometry as a point isotropic source to the DATA card section. Hereby, it is worth mentioning that all the simulation studies were performed using Lenovo® ThinkStation-P620/30E0008QUS Workstation-1x AMD-Ryzen, Threadripper PRO Hexadeca-core (16 Core) 3955WX 3.90 GHz −32 GB DDR4 SDRAM RAM.

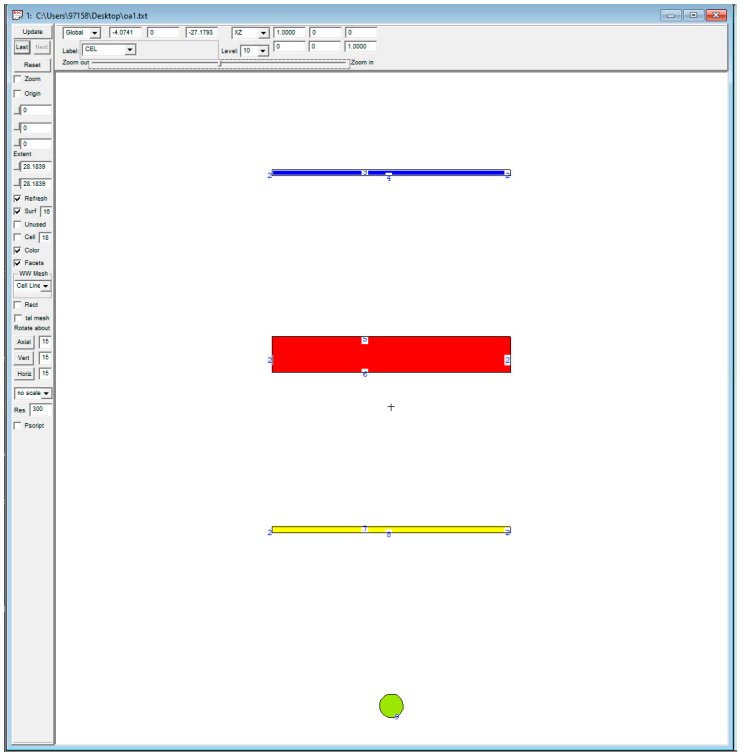

(**a**)

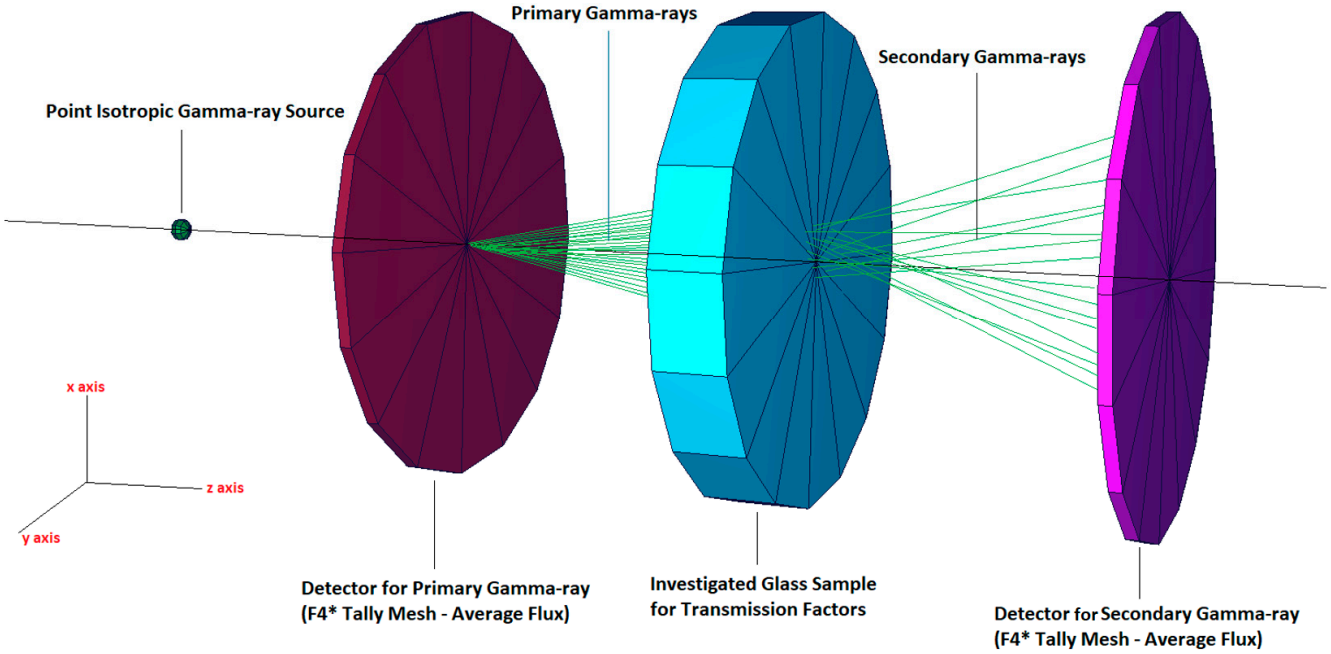

(**b**)

Figure 1. (**a**) 2-D view of designed MCNPX simulation setup (**b**) 3-D illustration of designed MCNPX setup (2-D and 3-D views were obtained from MCNPX Visual Editor VisedX22S).

3. Results and Discussions

Five different glass samples based on the Bi_2O_3–TeO_2–Na_2O–TiO_2–ZnO system were thoroughly studied in order to determine their basic shielding characteristics against ionizing gamma rays with an energy range of 0.015–15 MeV. It is well known that a material's gamma ray shielding competency is directly related to the density and atomic structure. Therefore, the shielding material lead (Pb) is the most preferable shielding material in

nuclear and medical radiation facilities worldwide. However, it has been aimed to alternate Pb with some ecofriendly, nontoxic, and cheaper shield materials, such as glasses and some superalloys to overcome the abovementioned disadvantages. Next, we determined one of the most important density-dependent gamma ray shielding parameters, namely, the linear attenuation coefficient (cm^{-1}). The term linear attenuation coefficient (μ) is a constant parameter representing the proportion of incoming photons that are attenuated in a monoenergetic beam per unit thickness of a material. The linear attenuation coefficient increases as the absorbing substance's atomic number and physical density rise. Figure 2 shows the variation of μ values as a function of incident gamma ray energy (MeV). As can be seen, the μ values' attitude varied according to the gamma ray energy area. A considerable decrease in the low energy area was observed as a consequence of the photoelectric effect's supremacy. The decrement continued in the midenergy area; however, the degree of decrement became smoother owing to Compton scattering dominance. After performing the linear attenuation coefficient calculations, it was determined that the S5 sample had the most significant values at each energy value. However, the acquired data indicate that there were no significant numerical differences amongst the samples investigated in the high energy range. The primary reason for this is that the differences in glass compositions were not chemically rigid, so the average total glass density change between S1 and S5 samples is 0.8 g/cm^3.

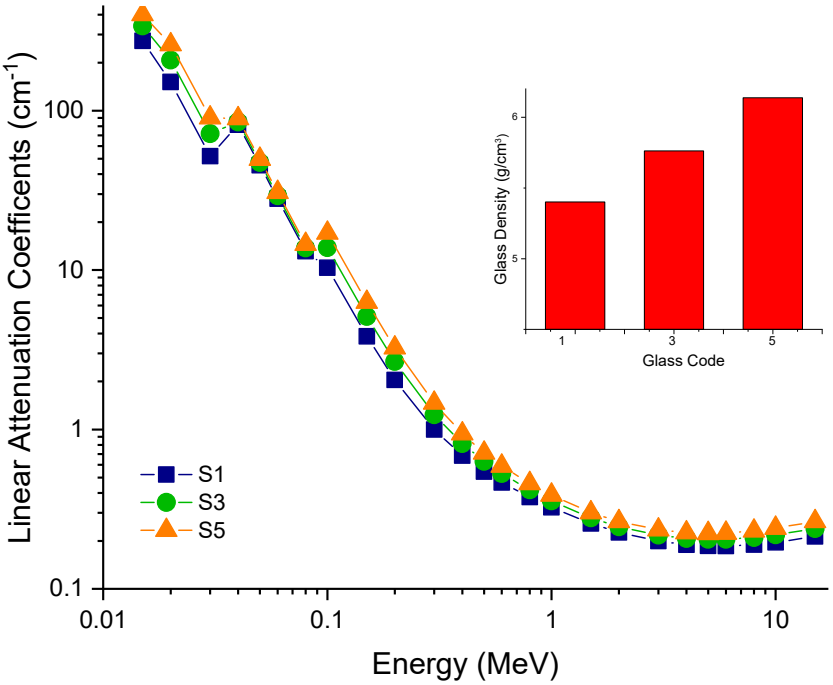

Figure 2. Variations of linear attenuation coefficient (cm^{-1}) with photon energy (MeV) for all S1–S5 glasses.

Figure 2 also describes the variation of the investigated glass densities. As can be observed, the glass densities range between 5.401 g/cm^3 and 6.138 g/cm^3. The net difference in density of 0.737 g/cm^3 is due to a 15% mole substitution of TeO_2 for Bi_2O_3. A tenth value layer (TVL, $X_{1/10}$) calculation, which is essential in nuclear and medical radiation applications, will provide incredibly relevant and practically useable information for determining the adequacy of the shielding material to be utilized. The (TVL, $X_{1/10}$) may be used to construct another parameter that is comparable to the half value layer (HVL, $X_{1/2}$) and gives similar information in function. This parameter specifies the material thickness necessary to reduce the radiation intensity on the material by one tenth. Figure 3 shows the energy-dependent variation of one tenth of the thickness of the heavy metal oxide glasses studied. As can be seen, tenth value layer values have higher quantitative

values for the same energy values compared to half value layer values. This situation is expected, and there is a need for thicker shielding material to reduce the intensity of the radiation with a certain energy value to one tenth. Although these two parameters take different quantitative values for the same energy values, the results of the study show that the S5 sample also had the lowest values in one-tenth value thicknesses. According to the conclusions drawn from these two crucial characteristics, the S5 sample will give a minimum of half and one-tenth value thicknesses in any process operating in the 0.015–15 MeV photon energy range. This demonstrates that using the S5 sample among the glass samples evaluated delivers the most benefit with the least expense and physical area occupied by the glass shield sample. Following the first interaction of the radiation with the shielding material and its penetration into the interior regions, individual interactions between the photon and the material atoms began within the material. The incoming radiation lost energy as a result of these interactions, and complete absorption happened when the energy reduced to zero.

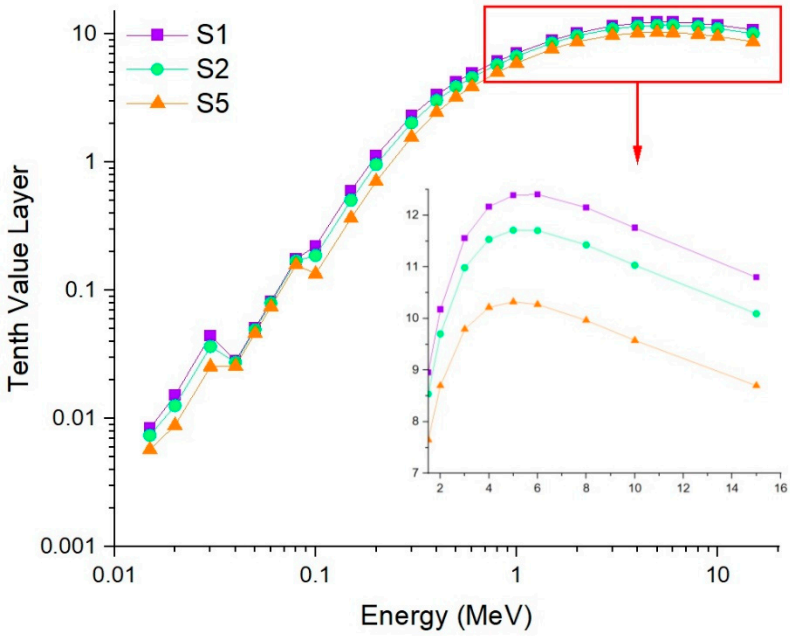

Figure 3. Variations of tenth value layer (cm) with photon energy (MeV) for all S1–S2–S5 glasses.

In order to evaluate the effective atomic number (Z_{eff}) of the investigated glasses, the ACS and ECS values had to be computed as radiation shielding parameters. The variation of the ACS as function of the incident photon energy is shown in Figure 4, while the variation of the ECS is shown in Figure 5. From Figures 4 and 5, it is seen that the ACS and ECS values decrease with increasing photon energy. In addition, the values of the ACS parameter are greater than that of the ECS parameter for all glasses. This may be attributed to the fact that the probability of total electronic interaction in any material of incident photons being lower than the probability of total atomic interaction.

According to Equation (5), values of the Z_{eff} values of the investigated (S1–S5) glasses were computed. Figure 6 shows the variations of effective atomic number (Z_{eff}) with photon energy (MeV). Due to the preponderance of photoelectric contact mechanisms in this region, the highest values of Z_{eff} were recorded in this area. A significant increase in Z_{eff} was seen in the lowest energy range of this behavior, owing to the increase in $Z_{Bi} = 83$ in the glass matrix. Following that, the Z_{eff} values in the intermediate zone decreased dramatically due to the prevalence of Compton scattering. Finally, in the most energy-intensive location, the development of Z_{eff} was seen again as a result of the majority of the phenomena associated with steam generation. This guarantees that the S5 with the biggest m has the highest possible Z_{eff}.

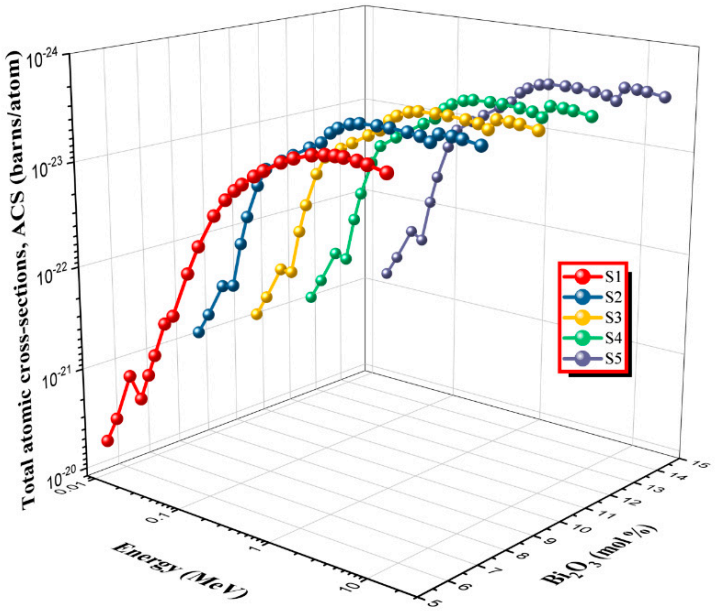

Figure 4. Variations of total atomic cross sections with photon energy (MeV) for all S1–S5 glasses.

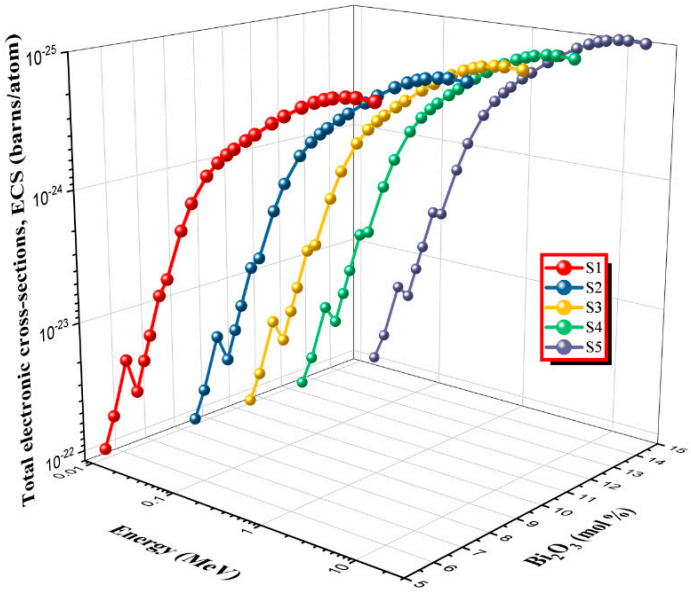

Figure 5. Variations of total atomic cross sections with photon energy (MeV) for all S1–S5 glasses.

Finally, another critical parameter for shielding materials, namely, gamma ray transmission factor (TF) values were determined for S1, S2, S3, S4, and S5 glass samples for various well-known radioisotope energies such as 0.0086 MeV (Ga-67), 0.0093 MeV (Ga-67), 0.0144 MeV (Co-57), 0.0230 MeV (In-111), 0.0532 MeV (Ba-133), 0.0710 MeV (Tl-201), 0.0796 MeV (Ba-133), 0.0810 MeV (Ba-133), 0.1221 MeV (Co-57), 0.1350 MeV (Tl-201), 0.1365 MeV (Co-57), 0.1405 MeV (Tc-99m), 0.1670 MeV (Tl-201), 0.1710 MeV (In-111), 0.1840 MeV (ga-67), 0.2450 MeV (In-111), 0.2764 MeV (Ba-133), 0.2843 MeV (I-131), 0.3029 MeV (Ba-133), 0.3201 MeV (Cr-51), 0.3560 MeV (Ba-133), 0.3645 MeV (I-131), 0.3838 MeV (Ba-133), 0.5110 MeV (Co-58), 0.6370 MeV (I-131), 0.6617 MeV (Cs-137), 0.7229 MeV (I-131), 0.8108 MeV (Co-58), 1.1732 MeV (Co-60), and 1.3325 MeV (Co-60).

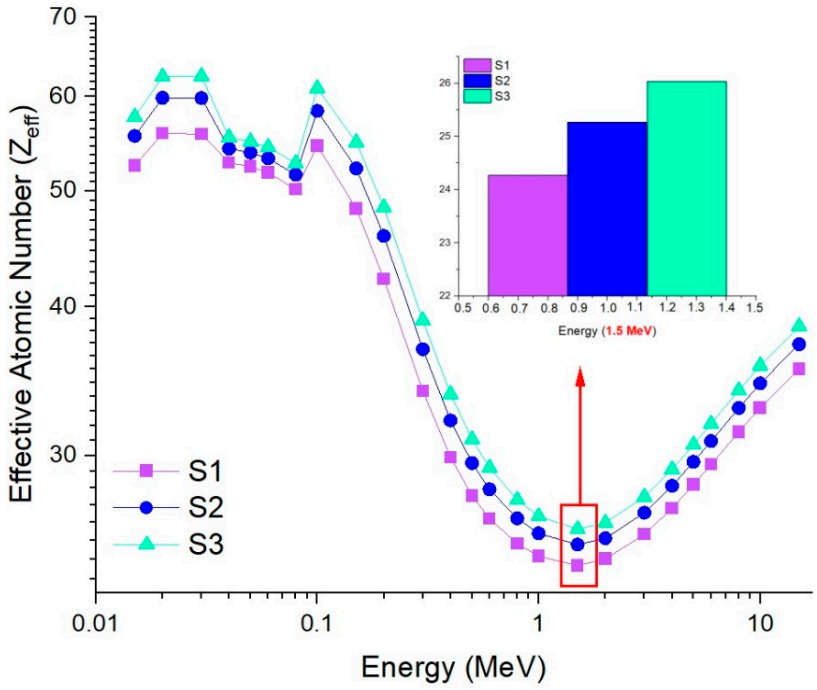

Figure 6. Variations of effective atomic number (Z_{eff}) with photon energy (MeV) for all S1–S2–S5 glasses.

TF values of the studied glasses were investigated in two steps. First, we determined the TF factors of S1, S2, S3, S4, and S5 samples at different glass thicknesses, respectively. Figure 7 depicts the TFs of investigated glasses as a function of used radioisotope energy (MeV) at different glass thicknesses (i.e., 0.5 cm, 1cm, and 3 cm). As can be observed, the transmission factor increased proportionately as the radioisotope energy increased from 0.0086 MeV to 1.3326 MeV. The glass samples had the lowest TF values in the low energy area for all the thicknesses. This is due to the great attenuation capabilities of these dense samples against low energy gamma rays. However, a distinct separation occurred around 0.1 MeV. After 0.1 MeV, glass samples began to respond differently in the context of incoming gamma rays at different thicknesses. The maximum attenuation (and minimum transmission) values were reported at 3 cm of glass thickness for all investigated glass samples. This condition is explained by the influence of shield thickness on the attenuation capabilities of any shielding material, which implies that increasing shield thickness increases incoming gamma ray attenuation. Next, the TF values of the examined glasses were comprehensively evaluated by comparing their attenuation capabilities throughout a range of glass thicknesses, such as 0.5 cm, 1 cm, 1.5 cm, 2 cm, 2.5 cm, and 3 cm, respectively.

Table 2 shows the comparison of the glass transmission factors (TFs) as a function of used radioisotope energy (MeV) for different glass thicknesses. As it is seen, TF values changed as a function of increasing incident gamma ray energy at all the thicknesses. Moreover, the minimum TF values were reported at 3 cm glass thickness for all the glass samples. However, S5 sample showed minimum transmission behavior at all the glass thicknesses used. According to previous studies in the literature, increasing the percentage of Bi_2O_3 in the glass composition may be an efficient solution of reducing the gamma radiation incidence on the material [38–41]. The findings of this study, which contributed to past studies, also indicate that glass structures with a larger Bi_2O_3 contribution had a higher density and hence better gamma ray reduction capabilities.

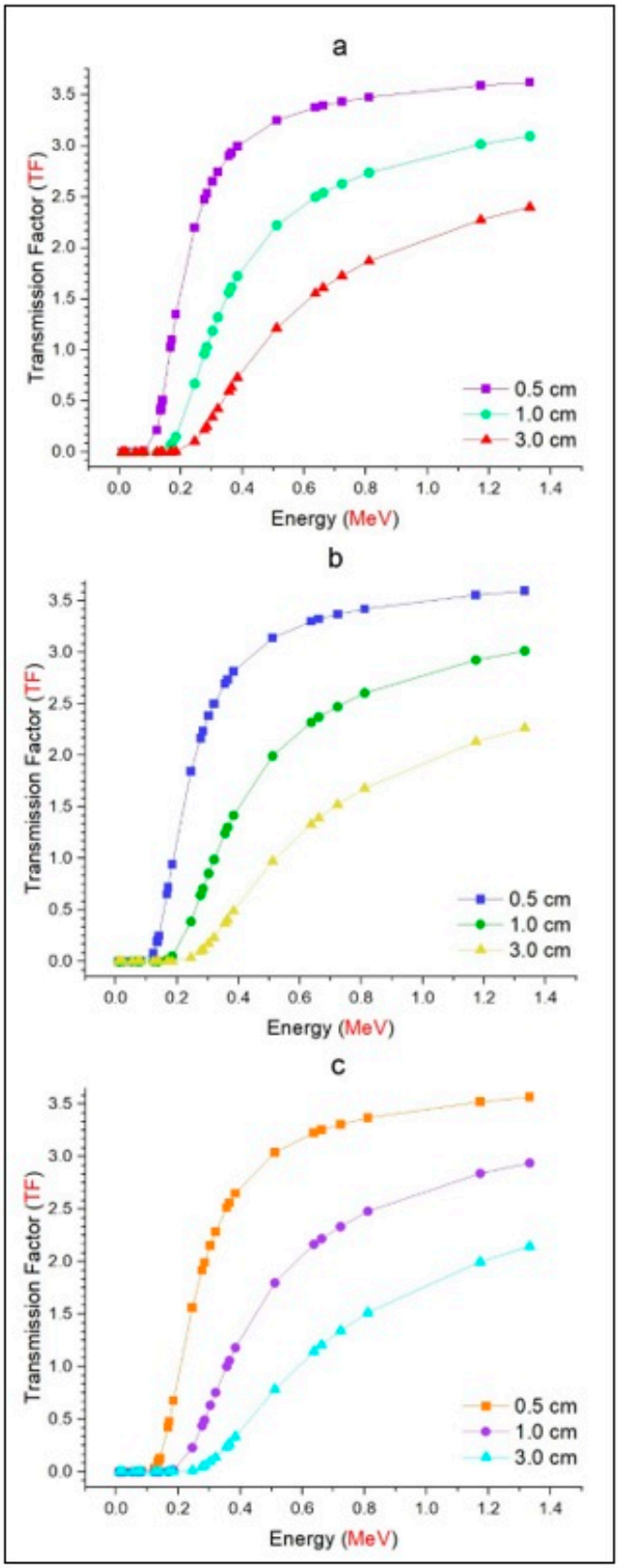

Figure 7. Transmission factors (**TFs**) of investigated glasses (**a**) S1, (**b**) S3, and (**c**) S5 as a function of used radioisotope energy (MeV) at different glass thicknesses.

Table 2. Comparison of the glass transmission factors (TFs) as a function of used radioisotope energy (MeV) for different glass thicknesses.

	Transmission Factors												
	Energy (MeV)	**0.5 m**	**1 cm**	**1.5 cm**	**2 cm**	**2.5 cm**	**3 cm**		**0.5 m**	**1 cm**	**1.5 cm**	**2 cm**	**2.5 cm**	**3 cm**
S1	**0.009**	0.000	0.000	0.000	0.000	0.000	0.000	**S2**	0.000	0.000	0.000	0.000	0.000	0.000
	0.009	0.000	0.000	0.000	0.000	0.000	0.000		0.000	0.000	0.000	0.000	0.000	0.000
	0.014	0.000	0.000	0.000	0.000	0.000	0.000		0.000	0.000	0.000	0.000	0.000	0.000
	0.023	0.000	0.000	0.000	0.000	0.000	0.000		0.000	0.000	0.000	0.000	0.000	0.000
	0.053	0.000	0.000	0.000	0.000	0.000	0.000		0.000	0.000	0.000	0.000	0.000	0.000
	0.071	0.001	0.000	0.000	0.000	0.000	0.000		0.001	0.000	0.000	0.000	0.000	0.000
	0.080	0.007	0.000	0.000	0.000	0.000	0.000		0.006	0.000	0.000	0.000	0.000	0.000
	0.081	0.009	0.000	0.000	0.000	0.000	0.000		0.008	0.000	0.000	0.000	0.000	0.000
	0.122	0.214	0.010	0.001	0.000	0.000	0.000		0.121	0.003	0.000	0.000	0.000	0.000
	0.135	0.411	0.041	0.004	0.000	0.000	0.000		0.264	0.017	0.001	0.000	0.000	0.000
	0.136	0.437	0.046	0.005	0.000	0.000	0.000		0.285	0.020	0.001	0.000	0.000	0.000
	0.141	0.509	0.064	0.008	0.001	0.000	0.000		0.341	0.029	0.002	0.000	0.000	0.000
	0.167	1.027	0.261	0.068	0.017	0.004	0.001		0.794	0.154	0.030	0.005	0.001	0.000
	0.171	1.102	0.303	0.082	0.022	0.006	0.002		0.868	0.183	0.040	0.008	0.002	0.000
	0.184	1.349	0.451	0.149	0.050	0.017	0.005		1.102	0.301	0.083	0.022	0.005	0.001
	0.245	2.198	1.216	0.669	0.363	0.194	0.107		1.989	0.992	0.493	0.239	0.119	0.058
	0.276	2.476	1.548	0.961	0.594	0.365	0.219		2.297	1.331	0.767	0.439	0.246	0.139
	0.284	2.535	1.622	1.029	0.653	0.409	0.253		2.369	1.408	0.831	0.489	0.284	0.165
	0.303	2.652	1.781	1.187	0.790	0.522	0.342		2.497	1.578	0.988	0.616	0.382	0.233
	0.320	2.745	1.911	1.321	0.909	0.621	0.425		2.602	1.716	1.123	0.734	0.473	0.304
	0.356	2.903	2.135	1.562	1.138	0.829	0.595		2.784	1.965	1.374	0.959	0.665	0.458
	0.364	2.932	2.179	1.615	1.192	0.873	0.637		2.821	2.016	1.430	1.010	0.710	0.496
	0.384	2.994	2.275	1.724	1.298	0.973	0.730		2.891	2.119	1.545	1.120	0.810	0.580
	0.511	3.249	2.695	2.221	1.826	1.494	1.215		3.187	2.587	2.091	1.683	1.344	1.070
	0.637	3.376	2.913	2.497	2.140	1.829	1.555		3.333	2.834	2.396	2.025	1.704	1.423
	0.662	3.394	2.945	2.539	2.189	1.881	1.609		3.353	2.871	2.442	2.077	1.761	1.484
	0.723	3.433	3.010	2.628	2.288	1.988	1.727		3.395	2.945	2.540	2.191	1.877	1.605
	0.811	3.476	3.090	2.737	2.414	2.130	1.872		3.445	3.032	2.660	2.322	2.023	1.763
	1.173	3.591	3.291	3.014	2.752	2.503	2.275		3.574	3.257	2.963	2.685	2.424	2.191
	1.332	3.622	3.352	3.093	2.847	2.614	2.400		3.606	3.321	3.047	2.791	2.548	2.324

	Transmission Factors												
	Energy (MeV)	**0.5 m**	**1 cm**	**1.5 cm**	**2 cm**	**2.5 cm**	**3 cm**		**0.5 m**	**1 cm**	**1.5 cm**	**2 cm**	**2.5 cm**	**3 cm**
S3	**0.009**	0.000	0.000	0.000	0.000	0.000	0.000	**S4**	0.000	0.000	0.000	0.000	0.000	0.000
	0.009	0.000	0.000	0.000	0.000	0.000	0.000		0.000	0.000	0.000	0.000	0.000	0.000
	0.014	0.000	0.000	0.000	0.000	0.000	0.000		0.000	0.000	0.000	0.000	0.000	0.000
	0.023	0.000	0.000	0.000	0.000	0.000	0.000		0.000	0.000	0.000	0.000	0.000	0.000
	0.053	0.000	0.000	0.000	0.000	0.000	0.000		0.000	0.000	0.000	0.000	0.000	0.000
	0.071	0.000	0.000	0.000	0.000	0.000	0.000		0.000	0.000	0.000	0.000	0.000	0.000
	0.080	0.005	0.000	0.000	0.000	0.000	0.000		0.005	0.000	0.000	0.000	0.000	0.000
	0.081	0.007	0.000	0.000	0.000	0.000	0.000		0.007	0.000	0.000	0.000	0.000	0.000
	0.122	0.079	0.001	0.000	0.000	0.000	0.000		0.058	0.001	0.000	0.000	0.000	0.000
	0.135	0.186	0.008	0.000	0.000	0.000	0.000		0.145	0.005	0.000	0.000	0.000	0.000
	0.136	0.203	0.010	0.000	0.000	0.000	0.000		0.159	0.006	0.000	0.000	0.000	0.000
	0.141	0.250	0.015	0.001	0.000	0.000	0.000		0.197	0.009	0.000	0.000	0.000	0.000
	0.167	0.651	0.103	0.017	0.002	0.000	0.000		0.562	0.078	0.010	0.001	0.000	0.000
	0.171	0.718	0.124	0.022	0.003	0.001	0.000		0.626	0.094	0.015	0.002	0.000	0.000
	0.184	0.942	0.217	0.051	0.011	0.003	0.001		0.838	0.171	0.035	0.007	0.001	0.000
	0.245	1.845	0.849	0.387	0.173	0.081	0.036		1.743	0.756	0.324	0.137	0.059	0.025
	0.276	2.164	1.181	0.642	0.344	0.182	0.098		2.075	1.082	0.561	0.286	0.146	0.075
	0.284	2.235	1.260	0.707	0.390	0.212	0.117		2.147	1.159	0.624	0.330	0.174	0.093
	0.303	2.384	1.434	0.853	0.508	0.298	0.175		2.302	1.337	0.772	0.442	0.248	0.140
	0.320	2.497	1.578	0.988	0.616	0.382	0.232		2.424	1.486	0.901	0.544	0.327	0.193

Table 2. *Cont.*

	Transmission Factors											
	Energy (MeV)	**0.5 m**	**1 cm**	**1.5 cm**	**2 cm**	**2.5 cm**	**3 cm**	**0.5 m**	**1 cm**	**1.5 cm**	**2 cm**	**2.5 cm**	**3 cm**
	0.356	2.694	1.839	1.242	0.836	0.558	0.373	2.630	1.750	1.157	0.760	0.496	0.320
	0.364	2.735	1.893	1.300	0.887	0.600	0.407	2.672	1.807	1.213	0.809	0.534	0.354
	0.384	2.814	2.007	1.417	0.997	0.700	0.489	2.758	1.925	1.334	0.920	0.627	0.430
	0.511	3.139	2.510	1.994	1.579	1.240	0.973	3.109	2.457	1.927	1.510	1.171	0.907
	0.637	3.299	2.776	2.320	1.940	1.612	1.330	3.277	2.737	2.269	1.883	1.551	1.268
	0.662	3.322	2.816	2.372	1.995	1.673	1.392	3.301	2.779	2.320	1.941	1.612	1.331
	0.723	3.368	2.896	2.472	2.111	1.797	1.523	3.351	2.862	2.432	2.065	1.745	1.467
	0.811	3.421	2.990	2.604	2.257	1.951	1.680	3.406	2.962	2.564	2.213	1.902	1.629
	1.173	3.556	3.230	2.925	2.636	2.372	2.132	3.546	3.214	2.899	2.607	2.338	2.095
	1.332	3.594	3.299	3.014	2.749	2.497	2.265	3.586	3.285	2.994	2.723	2.464	2.232
	Transmission Factors						
	Energy (MeV)	**0.5 m**	**1 cm**	**1.5 cm**	**2 cm**	**2.5 cm**	**3 cm**
	0.0086	0.0000	0.0000	0.0000	0.0000	0.0000	0.0000
	0.0093	0.0000	0.0000	0.0000	0.0000	0.0000	0.0000
	0.0144	0.0000	0.0000	0.0000	0.0000	0.0000	0.0000
	0.0230	0.0000	0.0000	0.0000	0.0000	0.0000	0.0000
	0.0532	0.0000	0.0000	0.0000	0.0000	0.0000	0.0000
	0.0710	0.0003	0.0000	0.0000	0.0000	0.0000	0.0000
	0.0796	0.0037	0.0000	0.0000	0.0000	0.0000	0.0000
	0.0810	0.0050	0.0000	0.0000	0.0000	0.0000	0.0000
	0.1221	0.0324	0.0002	0.0000	0.0000	0.0000	0.0000
	0.1350	0.0921	0.0020	0.0000	0.0000	0.0000	0.0000
	0.1365	0.1011	0.0025	0.00003	0.0000	0.0000	0.0000
	0.1405	0.1301	0.0038	0.0001	0.0000	0.0000	0.0000
	0.1670	0.4227	0.0432	0.0040	0.0004	0.00003	0.00003
S5	**0.1710**	0.4784	0.0552	0.0062	0.0007	0.00003	0.00003
	0.1840	0.6758	0.1093	0.0173	0.0027	0.0004	0.00003
	0.2450	1.5604	0.6071	0.2286	0.0899	0.0339	0.0127
	0.2764	1.9171	0.9188	0.4355	0.2040	0.0970	0.0452
	0.2843	1.9902	0.9915	0.4911	0.2397	0.1185	0.0579
	0.3029	2.1534	1.1662	0.6314	0.3358	0.1776	0.0958
	0.3201	2.2848	1.3180	0.7538	0.4273	0.2370	0.1348
	0.3560	2.5129	1.5928	1.0020	0.6243	0.3877	0.2363
	0.3645	2.5586	1.6526	1.0579	0.6725	0.4237	0.2649
	0.3838	2.6503	1.7764	1.1800	0.7796	0.5107	0.3330
	0.5110	3.0380	2.3395	1.7971	1.3693	1.0352	0.7831
	0.6370	3.2264	2.6540	2.1653	1.7613	1.4272	1.1449
	0.6617	3.2547	2.6972	2.2176	1.8216	1.4873	1.2062
	0.7229	3.3084	2.7894	2.3331	1.9507	1.6241	1.3425
	0.8108	3.3693	2.8979	2.4795	2.1109	1.7939	1.5160
	1.1732	3.5225	3.1716	2.8400	2.5294	2.2529	1.9987
	1.3325	3.5671	3.2455	2.9392	2.6507	2.3865	2.1460

4. Conclusions

Investigating the possibility for reinforced glasses to be utilized for a variety of applications in radiation fields is a hot topic that researchers have been focusing on in recent years. While this situation has benefited from the development of novel glass combinations and the material sciences literature in recent years, it continues to enable the development of the highest radiation protection conditions that can be achieved. In the current work, a detailed investigation of the gamma radiation shielding competencies and gamma radiation transmission factors (TFs) of tellurite glasses in the form of Bi_2O_3–TeO_2–Na_2O–TiO_2–ZnO with a density in the range between 5.401 g/cm^3 and 6.138 g/cm^3. This investigation was performed using Phys-X/PSD software and MCNPX Monte Carlo simulations. The re-

sults reveal that the (LAC, μ) values were increased with increasing the Bi_2O_3 content in the investigated (S1-S5) glasses. Generally, the LAC followed the trend as: $(LAC)_{S1} < (LAC)_{S2} < (LAC)_{S3} < (LAC)_{S4} < (LAC)_{S5}$. The (TVL, $X_{1/10}$) values of the investigated samples were decreased as the Bi_2O_3 content as well as density increased: $(TVL, X_{1/10})_{S1} > (TVL, X_{1/10})_{S2} > (TVL, X_{1/10})_{S3} > (TVL, X_{1/10})_{S4} > (TVL, X_{1/10})_{S5}$. The Z_{eff} parameter of the investigated S1-S5 glasses is similar to the LAC parameter. The transmission factor (TF) increases proportionately as the radioisotope energy increases from 0.0086 MeV to 1.3326 MeV. The glass samples had the lowest TF values in the low energy area for all the thicknesses. The maximum attenuation (and minimum transmission) values were reported at 3 cm of glass thickness for all investigated glass samples. The S5 sample showed minimum transmission behavior at all the glass thicknesses used. The primary objective of this study was to investigate the synergistic behavioral changes that occur as a result of various levels of Bi_2O_3 heavy metal oxide structure in the glass, as indicated by a literature review. Although this study focused on the glass samples and their shielding capabilities as a function of the quantity of Bi_2O_3, additional aspects such as mechanical, thermal, and cost analyses that are relevant to use conditions may be explored in future studies to provide a more comprehensive view.

Author Contributions: Conceptualization, H.O.T., G.A., H.M.H.Z. and S.A.M.I.; methodology, F.T.A. and H.O.T.; software, H.O.T., H.M.H.Z. and A.E.; validation, S.A.M.I., Y.S.R. and A.E.; formal analysis, Y.S.R., H.M.H.Z. and G.S.; investigation, F.T.A.; resources, G.S. and D.S.B.; data curation, G.A., S.A.M.I. and A.E.; writing—original draft preparation, H.O.T., G.S., Y.S.R. and D.S.B.; writing—review and editing, H.M.H.Z., D.S.B., S.A.M.I. and A.E.; visualization, Y.S.R. and G.S.; supervision, G.A., H.M.H.Z. and F.T.A.; project administration, H.O.T. and S.A.M.I.; The researcher (H.M.H.Z.) is funded by a scholarship under the Joint (Executive Program between Egypt and Russia). The work of A.E. and the APC was covered by "Dunarea de Jos" University of Galati, Romania. All authors have read and agreed to the published version of the manuscript.

Funding: This work was performed under Princess Nourah bint Abdulrahman University Researchers Supporting Project Number (PNURSP2022R149), Princess Nourah bint Abdulrahman University, Riyadh, Saudi Arabia. The authors express their sincere gratitude to Princess Nourah bint Abdulrahman University.

Institutional Review Board Statement: Not applicable.

Informed Consent Statement: Not applicable.

Data Availability Statement: The data presented in this study are available on request from the corresponding author.

Acknowledgments: The authors express their sincere gratitude to Princess Nourah bint Abdulrahman University.

Conflicts of Interest: The authors declare no conflict of interest.

References

1. Fares, H.; Jlassi, I.; Elhouichet, H.; Férid, M. Investigations of thermal, structural and optical properties of tellurite glass with WO3 adding. *J. Non-Cryst. Solids* **2014**, *396–397*, 1–7. [CrossRef]
2. Singh, V.P.; Badiger, N.; Kaewkhao, J. Radiation shielding competence of silicate and borate heavy metal oxide glasses: Comparative study. *J. Non-Cryst. Solids* **2014**, *404*, 167–173. [CrossRef]
3. Waly, E.-S.A.; Al-Qous, G.S.; Bourham, M.A. Shielding properties of glasses with different heavy elements additives for radiation shielding in the energy range 15–300 keV. *Radiat. Phys. Chem.* **2018**, *150*, 120–124. [CrossRef]
4. Rachniyom, W.; Chaiphaksa, W.; Limkitjaroeanporn, P.; Tuschaoen, S.; Sangwaranatee, N.; Kaewkhao, J. Effect of Bi2O3 on radiation shielding properties of glasses from coal fly ash. *Mater. Today Proc.* **2018**, *5*, 14046–14051. [CrossRef]
5. Prabhu, N.; Hegde, V.; Sayyed, M.; Agar, O.; Kamath, S.D. Investigations on structural and radiation shielding properties of Er^{3+} doped zinc bismuth borate glasses. *Mater. Chem. Phys.* **2019**, *230*, 267–276. [CrossRef]
6. Halimah, M.; Azuraida, A.; Ishak, M.; Hasnimulyati, L. Influence of bismuth oxide on gamma radiation shielding properties of boro-tellurite glass. *J. Non-Cryst. Solids* **2019**, *512*, 140–147. [CrossRef]
7. Kavaz, E.; Tekin, H.O.; Yorgun, N.Y.; Özdemir, Ö.F.; Sayyed, M. Structural and nuclear radiation shielding properties of bauxite ore doped lithium borate glasses: Experimental and Monte Carlo study. *Radiat. Phys. Chem.* **2019**, *162*, 187–193. [CrossRef]

8. Kirdsiri, K.; Kaewkhao, J.; Chanthima, N.; Limsuwan, P. Comparative study of silicate glasses containing Bi_2O_3, PbO and BaO: Radiation shielding and optical properties. *Ann. Nucl. Energy* **2011**, *38*, 1438–1441. [CrossRef]
9. Wagh, A.; Sayyed, M.; Askin, A.; Özpolat, Ö.F.; Şakar, E.; Lakshminarayana, G.; Kamath, S.D. Influence of RE oxides (Eu^{3+}, Sm^{3+}, Nd^{3+}) on gamma radiation shielding properties of lead fluoroborate glasses. *Solid State Sci.* **2019**, *96*, 105959. [CrossRef]
10. Wilson, M. Optimization of the radiation shielding capabilities of bismuth-borate glasses using the genetic algorithm. *Mater. Chem. Phys.* **2019**, *224*, 238–245. [CrossRef]
11. Yasmin, S.; Barua, B.S.; Khandaker, M.U.; Chowdhury, F.-U.-Z.; Rashid, A.; Bradley, D.A.; Olatunji, M.A.; Kamal, M. Studies of ionizing radiation shielding effectiveness of silica-based commercial glasses used in Bangladeshi dwellings. *Results Phys.* **2018**, *9*, 541–549. [CrossRef]
12. Sayyed, M. Bismuth modified shielding properties of zinc boro-tellurite glasses. *J. Alloys Compd.* **2016**, *688*, 111–117. [CrossRef]
13. Çelikbilek, M.; Ersundu, A.; Solak, N.; Aydin, S. Investigation on thermal and microstructural characterization of the TeO_2–WO_3 system. *J. Alloys Compd.* **2011**, *509*, 5646–5654. [CrossRef]
14. Moiseev, A.; Dorofeev, V.; Chilyasov, A.; Kraev, I.; Churbanov, M.; Kotereva, T.; Pimenov, V.; Snopatin, G.; Pushkin, A.; Gerasimenko, V.; et al. Production and properties of high purity TeO_2–ZnO–Na_2O–Bi_2O_3 and TeO_2–WO_3–La_2O_3–MoO_3 glasses. *Opt. Mater.* **2011**, *33*, 1858–1861. [CrossRef]
15. Dorofeev, V.; Moiseev, A.; Churbanov, M.; Snopatin, G.; Chilyasov, A.; Kraev, I.; Lobanov, A.; Kotereva, T.; Ketkova, L.; Pushkin, A.; et al. High-purity TeO_2–WO_3–(La_2O_3,Bi_2O_3) glasses for fiber-optics. *Opt. Mater.* **2011**, *33*, 1911–1915. [CrossRef]
16. Upender, G.; Ramesh, S.; Prasad, M.; Sathe, V.; Mouli, V. Optical band gap, glass transition temperature and structural studies of $(100-2x)TeO_{2-x}Ag_2O_{-x}WO_3$ glass system. *J. Alloys Compd.* **2010**, *504*, 468–474. [CrossRef]
17. Gunha, J.; Somer, A.; Gonçalves, A.; Sabino, S.D.R.; El-Mallawany, R.; Jacinto, C.; Novatski, A. Non-isothermal crystallization of TeO_2-Na_2O-TiO_2 glasses. *J. Non-Cryst. Solids* **2019**, *524*, 119655. [CrossRef]
18. Manning, S.; Ebendorff-Heidepriem, H.; Monro, T. Ternary tellurite glasses for the fabrication of nonlinear optical fibres. *Opt. Mater. Express* **2012**, *2*, 140–152. [CrossRef]
19. Sayyed, M.; Elhouichet, H. Variation of energy absorption and exposure buildup factors with incident photon energy and penetration depth for boro-tellurite (B_2O_3-TeO_2) glasses. *Radiat. Phys. Chem.* **2017**, *130*, 335–342. [CrossRef]
20. Elkhoshkhany, N.; Mohamed, H.M.; Yousef, E.S. UV–Vis-NIR spectroscopy, structural and thermal properties of novel oxyhalide tellurite glasses with composition TeO_2-B_2O_3-$SrCl_2$-LiF-Bi_2O_3 for optical application. *Results Phys.* **2019**, *13*, 102222. [CrossRef]
21. Udovic, M.; Thomas, P.; Mirgorodsky, A.; Durand, O.; Soulis, M.; Masson, O.; Merle-Méjean, T.; Champarnaud-Mesjard, J. Thermal characteristics, Raman spectra and structural properties of new tellurite glasses within the Bi_2O_3–TiO_2–TeO_2 system. *J. Solid State Chem.* **2006**, *179*, 3252–3259. [CrossRef]
22. Halimah, M.K.; Daud, W.M.; Sidek, H.A.A.; Zaidan, A.W.; Zainal, A.S. Optical properties of ternary tellurite glasses. *Mater. Sci.-Pol.* **2010**, *28*, 173–180.
23. Lakshminarayana, G.; Sayyed, M.I.; Baki, S.O.; Lira, A.; Dong, M.G.; Bashar, K.A.; Kityk, I.V.; Mahdi, M.A. Borotellurite Glasses for Gamma-Ray Shielding: An Exploration of Photon Attenuation Coefficients and Structural and Thermal Properties. *J. Electron. Mater.* **2018**, *48*, 930–941. [CrossRef]
24. Lakshminarayana, G.; Bashar, K.; Baki, S.; Lira, A.; Caldiño, U.; Meza-Rocha, A.; Falcony, C.; Camarillo, E.; Kityk, I.; Mahdi, M. Er^{3+}/Dy^{3+} codoped B_2O_3-TeO_2-PbO-ZnO-Li_2O-Na_2O glasses: Optical absorption and fluorescence features study for visible and near-infrared fiber laser applications. *J. Non-Cryst. Solids* **2019**, *503-504*, 366–381. [CrossRef]
25. Sultana, K.A.; Islam, T.; Silva, J.A.; Turley, R.S.; Hernandez-Viezcas, J.A.; Gardea-Torresdey, J.L.; Noveron, J.C. Sustainable synthesis of zinc oxide nanoparticles for photocatalytic degradation of organic pollutant and generation of hydroxyl radical. *J. Mol. Liq.* **2020**, *307*, 112931. [CrossRef]
26. Beegam, A.; Prasad, P.; Jose, J.; Oliveira, M.; Costa, F.G.; Soares, A.M.; Gonçalves, P.; Trindade, T.; Kalarikkal, N.; Thomas, S.; et al. Environmental Fate of Zinc Oxide Nanoparticles: Risks and Benefits. In *Toxicology—New Aspects to This Scientific Conundrum*; Springer: Berlin/Heidelberg, Germany, 2016. [CrossRef]
27. Shimoji, N.; Hashimoto, T.; Nasu, H.; Kamiya, K. Non-linear optical properties of Li_2O–TiO_2–P_2O_5 glasses. *J. Non-Cryst. Solids* **2003**, *324*, 50–57. [CrossRef]
28. Gowda, V.V.; Reddy, C.N.; Radha, K.; Anavekar, R.; Etourneau, J.; Rao, K. Structural investigations of sodium diborate glasses containing PbO, Bi_2O_3 and TeO_2: Elastic property measurements and spectroscopic studies. *J. Non-Cryst. Solids* **2007**, *353*, 1150–1163. [CrossRef]
29. Hirashima, H.; Arai, D.; Yoshida, T. Electrical Conductivity of PbO-P_2O_5-V_2O_5Glasses. *J. Am. Ceram. Soc.* **1985**, *68*, 486–489. [CrossRef]
30. Elliott, S.R.; Rao, C.; Thomas, J.M. The chemistry of the non-crystalline state. *Angew. Chem. Int. Ed.* **1986**, *25*, 31–46. [CrossRef]
31. Fong, W.; Bashar, K.; Baki, S.; Zaid, M.; Goh, B.; Mahdi, M. Thermal, structural and optical properties of Bi_2O_3-Na_2O-TiO_2-ZnO-TeO_2 glass system. *J. Non-Cryst. Solids* **2021**, *555*, 120621. [CrossRef]
32. Alım, B.; Şakar, E.; Baltakesmez, A.; Han, İ.; Sayyed, M.I.; Demir, L. Experimental investigation of radiation shielding performances of some important AISI-coded stainless steels: Part I. *Radiat. Phys. Chem.* **2020**, *166*, 108455. [CrossRef]
33. Zakaly, H.M.; Saudi, H.; Tekin, H.; Rashad, M.; Issa, S.A.; Rammah, Y.; Elazaka, A.; Hessien, M.; Ene, A. Glass fabrication using ceramic and porcelain recycled waste and lithium niobate: Physical, structural, optical and nuclear radiation attenuation properties. *J. Mater. Res. Technol.* **2021**, *15*, 4074–4085. [CrossRef]

34. Zakaly, H.M.; Ashry, A.; El-Taher, A.; Abbady, A.G.; Allam, E.A.; El-Sharkawy, R.M.; Mahmoud, M.E. Role of novel ternary nanocomposites polypropylene in nuclear radiation attenuation properties: In-depth simulation study. *Radiat. Phys. Chem.* **2021**, *188*, 109667. [CrossRef]
35. Şakar, E.; Özpolat, Ö.F.; Alım, B.; Sayyed, M.I.; Kurudirek, M. Phy-X/PSD: Development of a user friendly online software for calculation of parameters relevant to radiation shielding and dosimetry. *Radiat. Phys. Chem.* **2020**, *166*, 108496. [CrossRef]
36. Almatari, M.; Agar, O.; Altunsoy, E.; Kilicoglu, O.; Sayyed, M.; Tekin, H.O. Photon and neutron shielding characteristics of samarium doped lead alumino borate glasses containing barium, lithium and zinc oxides determined at medical diagnostic energies. *Results Phys.* **2019**, *12*, 2123–2128. [CrossRef]
37. RSICC Computer Code Collection. In MCNPX 'User's Manual Version 2.4.0. In *Monte Carlo N-Particle Transport Code System for Multiple and High Energy Applications*; Oak Ridge National Laboratory: Oak Ridge, TN, USA; Advanced Accelerator Applications Los Alamos National Laboratory: Los Alamos, NM, USA, 2002.
38. Lakshminarayana, G.; Issa, S.A.; Saddeek, Y.; Tekin, H.; Al-Buriahi, M.; Dong, M.; Lee, D.-E.; Yoon, J.; Park, T. Analysis of physical and mechanical traits and nuclear radiation transmission aspects of Gallium(III) trioxide constituting Bi_2O_3-B_2O_3 glasses. *Results Phys.* **2021**, *30*, 104899. [CrossRef]
39. Lakshminarayana, G.; Kumar, A.; Tekin, H.; Issa, S.A.; Al-Buriahi, M.; Dong, M.; Lee, D.-E.; Yoon, J.; Park, T. Probing of nuclear radiation attenuation and mechanical features for lithium bismuth borate glasses with improving Bi_2O_3 content for B_2O_3 + Li_2O amounts. *Results Phys.* **2021**, *25*, 104246. [CrossRef]
40. Kurtulus, R.; Kavas, T.; Akkurt, I.; Gunoglu, K.; Tekin, H.O.; Kurtulus, C. A comprehensive study on novel alumino-borosilicate glass reinforced with Bi_2O_3 for radiation shielding applications: Synthesis, spectrometer, XCOM, and MCNP-X works. *J. Mater. Sci. Mater. Electron.* **2021**, *32*, 13882–13896. [CrossRef]
41. Lakshminarayana, G.; Kumar, A.; Tekin, H.; Issa, S.A.; Al-Buriahi, M.; Lee, D.-E.; Yoon, J.; Park, T. Binary B_2O_3–Bi_2O_3 glasses: Scrutinization of directly and indirectly ionizing radiations shielding abilities. *J. Mater. Res. Technol.* **2020**, *9*, 14549–14567. [CrossRef]